



(This is a sample cover image for this issue. The actual cover is not yet available at this time.)

This article appeared in a journal published by Elsevier. The attached copy is furnished to the author for internal non-commercial research and education use, including for instruction at the authors institution and sharing with colleagues.

Other uses, including reproduction and distribution, or selling or licensing copies, or posting to personal, institutional or third party websites are prohibited.

In most cases authors are permitted to post their version of the article (e.g. in Word or Tex form) to their personal website or institutional repository. Authors requiring further information regarding Elsevier's archiving and manuscript policies are encouraged to visit:

<http://www.elsevier.com/copyright>



Contents lists available at SciVerse ScienceDirect

International Journal of Engineering Science

journal homepage: www.elsevier.com/locate/ijengsci

Effective properties of piezoelectric composites with parallelogram periodic cells

R. Guinovart-Díaz^{a,*}, P. Yan^b, R. Rodríguez-Ramos^a, J.C. López-Realpozo^a, C.P. Jiang^b, J. Bravo-Castillero^a, F.J. Sabina^c^a Facultad de Matemática y Computación, Universidad de La Habana, San Lázaro y L, Vedado, Habana 4, CP-10400, Cuba^b School of Aeronautic Science and Engineering, Beijing University of Aeronautics and Astronautics, Beijing 100191, China^c Instituto de Investigaciones en Matemáticas Aplicadas y en Sistemas Universidad Nacional Autónoma de México, Apartado Postal 20-726, Delegación de Álvaro Obregón, 01000 México, DF, Mexico

ARTICLE INFO

Article history:

Received 8 December 2011

Received in revised form 18 December 2011

Accepted 26 December 2011

Keywords:

Effective properties

Double periodic

Fibrous composites

Piezoelectric composites

ABSTRACT

In this work, a two-phase parallel fiber-reinforced periodic piezoelectric composite is considered wherein the constituents exhibit transverse isotropy. Simple closed-form formulae are obtained for the axial effective properties of the composites by means of the asymptotic homogenization method (AHM) and eigenfunction expansion-variational method (EEVM) for different types of parallelogram cells. Some numerical examples and comparisons with other theoretical results demonstrate that both methods are efficient for the analysis of composites with presence of parallelogram cells. The effects of the configuration of the cells on the effective properties are observed. In general, both models predict the monoclinic behavior of the composites.

© 2012 Elsevier Ltd. All rights reserved.

1. Introduction

Analytic expressions for piezoelectric effective coefficients of fibrous composites with isotropic elastic constituents for square and hexagonal cells under perfect contact condition at the interfaces are calculated in many previous works. In Bravo-Castillero, Guinovart-Díaz, Sabina, and Rodríguez-Ramos (2001), Sabina, Rodríguez-Ramos, Bravo-Castillero, and Guinovart-Díaz (2001), and Molkov and Pobedria (1985) analytical expressions for the effective properties are obtained using asymptotic homogenization method (AHM). In Golovchan and Nikltyuk (1981) a very attractive method is presented for the solution of the problem on the shear of a regular fibrous medium underlying which is the exact solution of the Laplace equation in a strip with an infinite number of circular holes. Only single, quite convergent series are used here. Recently, in Guinovart-Díaz et al. (2011) the effective elastic moduli of two-phase fibrous periodic composites are obtained for different types of parallelogram cells based on the AHM and making use of potential methods of a complex variable and properties of elliptic and related functions. The constituents exhibit transversely isotropic properties. A doubly periodic-parallelogram array of cylindrical inclusions under longitudinal shear is considered. The behavior of the shear elastic effective coefficient for different geometry arrays of the cell related to the angle of the fibers is studied. On the other hand, eigen-function expansion-variational method (EEVM) is applied in Rodríguez-Ramos et al. (2011) and Yan and Jiang (2010) in order to obtain

* Corresponding author.

E-mail addresses: guino@matcom.uh.cu (R. Guinovart-Díaz), yanpeng117@buaa.edu.cn (P. Yan), reinaldo@matcom.uh.cu (R. Rodríguez-Ramos), jclrealpozo@matcom.uh.cu (J.C. López-Realpozo), jiangchiping@buaa.edu.cn (C.P. Jiang), jbravo@matcom.uh.cu (J. Bravo-Castillero), fjs@mym.iimas.unam.mx (F.J. Sabina).

effective properties of cracked elastic solids and piezoelectric composites. Such approaches permitted obtaining values of the elastic and piezoelectric moduli for different angle of inclination of the cells.

In this work, micromechanical analysis methods are applied to unidirectional fiber piezoelectric composites with different cross angles of the cells to determine the homogenized piezoelectric properties of the composite. This research is inspired in recent publications (Guinovart-Díaz et al., 2011; Rodríguez-Ramos et al., 2011; Yan & Jiang, 2010; Yan, Jiang, Song, & Xu, 2010). In particular, this work compiles all piezoelectric average properties for the antiplane problem calculated by AHM and EEM for different geometry arrays of the cell in two-phase fibrous periodic composites. Since the theoretical fundamentals of both methods are in details developed in a separately form in previous works, a comparison between the results of the axial piezoelectric effective coefficients derived for both methods is convenient and it is presented here. Moreover, the difference of the present work with respect to other previous works consists in the computation of all effective coefficients for different parallelogram one-directional fiber distribution where the symmetry lines define a parallelepiped unit cell, representing the periodic microstructure of this fibrous composite. Though, to the best of our knowledge, real materials with parallelogram periodic cells are not available, such kind of composites are expected to be fabricated by the method developed by Boyd, Lagoudas, and Seo (2003). Furthermore, recently theoretical studies for composites with rhombic cell have been considered in Artioli, Bisegna, and Maceri (2010) and Nabi, Abhay, Ghodrat, and Chad (2008). On the other hand, such kind of composites is expected to have special use, due to the anisotropy induced by the parallelogram periodic fiber arrays. Such anisotropy makes it possible to obtain electric field in one direction by applying deformation on the composites in another direction or vice versa.

The effect of the geometry distributions and the angle of the fibers in the composite are analyzed. The results of this paper are mainly based on the impact of the fiber cross angles on the axial stiffness properties obtaining a composite characterized by 3 homogenized elastic coefficients (C_{44}^* , C_{55}^* , C_{45}^*); 3 homogenized piezoelectric coefficients (e_{14}^* , e_{15}^* , e_{24}^*) and 3 homogenized dielectric coefficients (κ_{11}^* , κ_{12}^* , κ_{22}^*). In particular, for rhombic periodic cells with 60° and 90° a composite with hexagonal and tetragonal crystal classes Royer and Dieulesaint (2000) respectively are obtained in Bravo-Castillero et al. (2001) and Sabina et al. (2001). The accuracy of the results from both micromechanics modeling procedures has been compared.

2. Asymptotic homogenization method (AHM)

Consider piezoelectric materials that respond linearly to changes in the mechanic and electric fields. A two-phase uniaxial reinforced material is considered here in which fibers and matrix have transversely isotropic properties; the axis of transverse symmetry coincides with the fiber direction, which is taken as the Ox_3 axis. The fiber cross-section is circular. Moreover, the fibers are periodically distributed without overlapping in directions parallel to the Ow_1 - and Ow_2 -axis, where $w_1 \neq 0$ and $w_2 \neq 0$ ($w_2 \neq \lambda w_1$, $\lambda \in \mathbb{R}$) are two complex numbers which define the parallelogram periodic cell of the two-phase composite. The composite consists of a parallelogram array of identical circular cylinders embedded in a homogeneous medium. The cylinders are infinitely long. As shown in Fig. 1, the infinitely extended doubly-periodic structure is obtained from a primitive cell which is repeated in the two directions, where w_1 and w_2 denote the two fundamental periods. The general period T_{nm} can be defined as $T_{nm} = nw_1 + mw_2$, where n and m are arbitrary integers.

Using the conventional indicial notation in which repeated subscripts are summed over the range of $i, j, k, l = 1, 2, 3$, the constitutive equations are

$$\sigma_{ij} = C_{ijkl} \varepsilon_{kl} - e_{kij} E_k, \quad D_i = e_{ikl} \varepsilon_{kl} + \kappa_{ik} E_k, \quad (1)$$

where σ_{ij} , ε_{ij} , E_i , and D_i are the stress tensor, strain tensor, electric field vector, and the electric displacement vector, respectively. The quantities C_{ijkl} , e_{kij} , κ_{ik} are the elastic stiffness tensor, the piezoelectric tensor, and the permittivity tensor, respectively. The divergence equations, which are the elastic equilibrium as the body forces are absent, and Gauss' law, are, respectively,

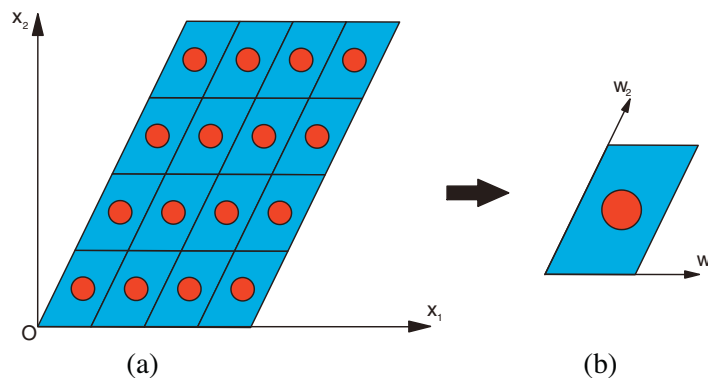


Fig. 1. The heterogeneous medium and extracted parallelogram periodic cell.

$$\sigma_{ij,j} = 0, \quad D_{i,i} = 0, \quad (2)$$

where the subscript comma denotes partial differentiation. The gradient equations, which are the strain–displacement equations and electric field–potential, are, respectively,

$$\varepsilon_{kl} = \frac{1}{2} \left(\frac{\partial u_k}{\partial x_l} + \frac{\partial u_l}{\partial x_k} \right), \quad E_i = -\phi_{,i} \quad (3)$$

where u_i and ϕ are the mechanical displacement and electric potential, respectively.

Substituting (1) and (3) into (2) we obtain a coupled system of partial differential equations with coefficients rapidly oscillating

$$(C_{ijkl}(\mathbf{y})u_{k,l} + e_{kij}(\mathbf{y})\phi_{,k})_{,j} = 0, \quad (e_{ikl}(\mathbf{y})u_{k,l} - \kappa_{ik}(\mathbf{y})\phi_{,k})_{,i} = 0 \quad \text{on } \Omega \quad (4)$$

The overall properties of the above periodic medium are sought by means of the well-known asymptotic homogenization method (AHM) (Bravo-Castillero et al., 2001; Sabina et al., 2001). $\mathbf{x} \in \Omega$ and $\mathbf{y} = \mathbf{x}/\varepsilon$, $\mathbf{y} \in Y$ denote the global and the local variables, where $\varepsilon = l/L$ is a small dimensionless parameter and L is a linear dimension of the body.

The system of Eq. (4) under suitable boundary conditions can be solved asymptotically posing the ansatz

$$\begin{aligned} \mathbf{u}(\mathbf{x}) &= \tilde{\mathbf{u}}(\mathbf{x}) + \varepsilon \tilde{\mathbf{u}}_1(\mathbf{x}, \mathbf{y}) + O(\varepsilon^2), \\ \varphi(\mathbf{x}) &= \tilde{\varphi}(\mathbf{x}) + \varepsilon \tilde{\varphi}_1(\mathbf{x}, \mathbf{y}) + O(\varepsilon^2), \end{aligned}$$

where $\tilde{\mathbf{u}}$ and $\tilde{\varphi}$ satisfy the homogenized system of differential equations

$$\begin{aligned} C_{ijkl}^* \tilde{u}_{l,kj} + e_{kij}^* \tilde{\varphi}_{,kj} &= 0, \\ e_{ikj}^* \tilde{u}_{i,kj} - \kappa_{jk}^* \tilde{\varphi}_{,kj} &= 0, \quad \text{on } \Omega \end{aligned} \quad (5)$$

and the asterisk denotes the overall property. The terms $\tilde{\mathbf{u}}_1$, $\tilde{\varphi}_1$ represent a correction of the $\tilde{\mathbf{u}}$, $\tilde{\varphi}$ respectively. The functions $\tilde{\mathbf{u}}_1$, $\tilde{\varphi}_1$ are found in combination of the functions $\mathbf{M}(\mathbf{y})$, $\mathbf{N}(\mathbf{y})$, $\mathbf{P}(\mathbf{y})$ and $\mathbf{Q}(\mathbf{y})$ (solution of the local problems) and the partial derivatives of the functions $\tilde{\mathbf{u}}$, $\tilde{\varphi}$.

By AHM, the original constitutive relations with rapidly oscillating material coefficients (4) are transformed into equivalent system (5) with constant coefficients \mathbf{C}^* , \mathbf{e}^* , $\mathbf{\kappa}^*$ which represent the elastic, piezoelectric and permittivity properties, respectively of an equivalent homogeneous medium and are called the effective coefficients of Ω .

The main problem to obtain such average formulae is to find the Y -periodic solutions of nine L_{pq} , I_p ($p, q = 1, 2, 3$) local problems on Y in terms of the fast variable \mathbf{y} (Bravo-Castillero et al., 2001; Sabina et al., 2001). The L_{pq} problem is formulated as seeking displacement ${}_{pq}M^{(\alpha)}(\mathbf{y})$ and potentials ${}_{pq}N^{(\alpha)}(\mathbf{y})$, in Y_α , $\alpha = 1, 2$, which are periodic functions of periods $w_1 = 1$, $w_2 = be^{i\Theta}$, b is the modulus of this complex number. In a similar way, the I_p problem is stated in terms of the displacement ${}_pP^{(\alpha)}(\mathbf{y})$ and potentials ${}_pQ^{(\alpha)}(\mathbf{y})$ with the same periods. The mathematical statement of both problems can be found in Bravo-Castillero et al. (2001).

Then, it follows that in terms of the fast variable \mathbf{y} , the appropriate periodic unit cell Y is taken as a regular parallelogram in the y_1y_2 -plane so that $Y = Y_1 \cup Y_2$ with $Y_1 \cap Y_2 = \emptyset$, where the domain Y_1 is occupied by the matrix and its complement Y_2 , a circle of radius R , is filled up with the fiber (Fig. 2). The common interface between the fiber and the matrix is denoted by Γ . Beside the use of subscript, matrix and fiber associated quantities are also referred below by means of superscripts in brackets (1) and (2), respectively.

Once the local problems are solved, the homogenized moduli C_{ijpq}^* , e_{kij}^* , κ_{ik}^* may be determined by using the following formulae:

$$\begin{aligned} C_{ijpq}^* &= \langle C_{ijpq} + C_{ijklpq}M_{k,l} + e_{kijpq}N_{,k} \rangle, & e_{ipq}^* &= \langle e_{ipq} + e_{iklpq}M_{k,l} - \kappa_{ikpq}N_{,k} \rangle, \\ e_{pij}^* &= \langle e_{pij} + C_{ijklp}P_{k,l} + e_{kijp}Q_{,k} \rangle, & \kappa_{ip}^* &= \langle \kappa_{ip} - e_{iklp}P_{k,l} + \kappa_{ikp}Q_{,k} \rangle \end{aligned} \quad (6)$$

where $\langle \bullet \rangle = \frac{1}{|\Omega|} \int_\Omega \bullet dX$.

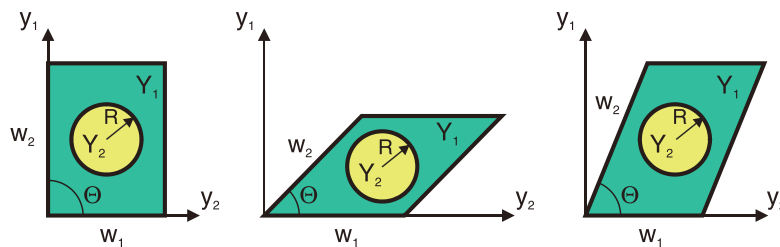


Fig. 2. Different unit cells – rectangle, rhombic and parallelogram.

Each local problem uncouples into sets of equations, i.e. plane-strain and antiplane-strain systems. The aim of the present work is the calculation of the axial effective moduli which are related to antiplane problems L_{13} , L_{23} , I_1 and I_2 (Bravo-Castilero et al., 2001; Sabina et al., 2001). The closed form formulae of the effective coefficients can be listed as follows

$$\begin{aligned} C_{13\alpha 3}^* - iC_{23\alpha 3}^* &= C_{1313}^{(1)}(\delta_{1\alpha} - i\delta_{2\alpha} - 2V_2\Pi_{1\alpha}), & e_{1\alpha 3}^* - ie_{2\alpha 3}^* &= \sqrt{C_{1313}^{(1)}\kappa_{11}^{(1)}}(E^{(1)}(\delta_{1\alpha} - i\delta_{2\alpha}) - 2V_2\Pi_{2\alpha}), \\ \kappa_{\alpha 1}^* - i\kappa_{\alpha 2}^* &= \kappa_{11}^{(1)}(\delta_{1\alpha} - i\delta_{2\alpha} + 2V_2\Pi_{3\alpha}), & e_{\alpha 13}^* - ie_{\alpha 23}^* &= \sqrt{C_{1313}^{(1)}\kappa_{11}^{(1)}}(E^{(1)}(\delta_{1\alpha} - i\delta_{2\alpha}) - 2V_2\Pi_{4\alpha}), \end{aligned} \quad (7)$$

where

$$\begin{aligned} \Pi_{1\alpha} &= \bar{a}_{1(\alpha 3)} + E^{(1)}\bar{b}_{1(\alpha 3)}, & \Pi_{2\alpha} &= E^{(1)}\bar{a}_{1(\alpha 3)} - \bar{b}_{1(\alpha 3)}, \\ \Pi_{3\alpha} &= E^{(1)}\bar{a}_{1(\alpha)} - \bar{b}_{1(\alpha)}, & \Pi_{4\alpha} &= \bar{a}_{1(\alpha)} + E^{(1)}\bar{b}_{1(\alpha)}, & E^{(\alpha)} &= e_{113}^{(\alpha)} / \sqrt{C_{1313}^{(\alpha)}\kappa_{11}^{(\alpha)}}, \end{aligned}$$

the over bar denotes complex conjugate numbers and $a_{1(\alpha 3)}$, $b_{1(\alpha 3)}$, $a_{1(\alpha)}$ and $b_{1(\alpha)}$ are solution of the infinite systems related to the local problems.

Numerical computation of the effective coefficients (7) requires a suitable algorithm. In order to obtain the unknown complex numbers $a_{1(\alpha 3)}$, $b_{1(\alpha 3)}$, $a_{1(\alpha)}$ and $b_{1(\alpha)}$ is necessary to solve the system of algebraic equations written in the form

$$\mathbf{X} = \mathcal{Z}^{-1}\mathcal{A}_{(\cdot)}, \quad (8)$$

where the vector $\mathbf{X}^t = (x_1, x_2, x_3, x_4)$, $a_{1(\cdot)} = x_1 + ix_2$, $b_{1(\cdot)} = x_3 + ix_4$ and the vector $\mathcal{A}_{(\cdot)}$ for different local problems is given by

$$\begin{aligned} \mathcal{A}_{(13)}^T &= (\chi_\rho, 0, \chi_s, 0), & \mathcal{A}_{(23)}^T &= (0, \chi_\rho, 0, \chi_s), & \mathcal{A}_{(1)}^T &= (\chi_{s\rho}^-, 0, \chi_{s\rho}^-, 0) & \text{and} & \mathcal{A}_{(2)}^T &= (0, \chi_{s\rho}^-, 0, \chi_{s\rho}^-), \\ \chi_\rho &= \frac{C_{1313}^{(1)} - C_{1313}^{(2)}}{C_{1313}^{(1)} + C_{1313}^{(2)}}, & \chi_s &= \frac{e_{113}^{(1)} - e_{113}^{(2)}}{e_{113}^{(1)} + e_{113}^{(2)}}, & \chi_{s\rho}^\pm &= \frac{E^{(1)} \pm E^{(2)}\sqrt{\rho t}}{1 + \rho}, & \chi_{ts}^\pm &= -\frac{1 \pm t}{E^{(1)} + E^{(2)}\sqrt{\rho t}}, \\ \rho &= C_{1313}^{(2)} / C_{1313}^{(1)}, & t &= \kappa_{11}^{(2)} / \kappa_{11}^{(1)}. \end{aligned} \quad (9)$$

Moreover, the numerical matrix \mathcal{Z} of 4×4 -order is defined by $\mathcal{Z} = \mathcal{K} + R^2\mathcal{J} - \mathcal{N}_1\mathcal{P}^{-1}\mathcal{N}_2$, R is the radius of the fiber,

$$\begin{aligned} \mathcal{K} &= \begin{pmatrix} 1 & 0 & \chi_{s\rho}^+ & 0 \\ 0 & 1 & 0 & \chi_{s\rho}^+ \\ 1 & 0 & \chi_{ts}^+ & 0 \\ 0 & 1 & 0 & \chi_{ts}^+ \end{pmatrix}, & \mathcal{J} &= \begin{pmatrix} \chi_\rho \begin{pmatrix} h_{11} + h_{12} & h_{21} - h_{22} \\ -(h_{21} + h_{22}) & h_{11} - h_{12} \end{pmatrix} & \chi_{s\rho}^- \begin{pmatrix} h_{11} + h_{12} & h_{21} - h_{22} \\ -(h_{21} + h_{22}) & h_{11} - h_{12} \end{pmatrix} \\ \chi_s \begin{pmatrix} h_{11} + h_{12} & h_{21} - h_{22} \\ -(h_{21} + h_{22}) & h_{11} - h_{12} \end{pmatrix} & \chi_{ts}^- \begin{pmatrix} h_{11} + h_{12} & h_{21} - h_{22} \\ -(h_{21} + h_{22}) & h_{11} - h_{12} \end{pmatrix} \end{pmatrix}, & h_{11} &= \Re\left\{\frac{\delta_1\bar{w}_2 - \delta_2\bar{w}_1}{w_1\bar{w}_2 - w_2\bar{w}_1}\right\}, & h_{12} &= \\ \Re\left\{\frac{\delta_1\bar{w}_2 - \delta_2\bar{w}_1}{w_1\bar{w}_2 - w_2\bar{w}_1}\right\}, & h_{21} &= \Im\left\{\frac{\delta_1\bar{w}_2 - \delta_2\bar{w}_1}{w_1\bar{w}_2 - w_2\bar{w}_1}\right\}, & h_{22} &= \Im\left\{\frac{\delta_1\bar{w}_2 - \delta_2\bar{w}_1}{w_1\bar{w}_2 - w_2\bar{w}_1}\right\}, & \delta_\alpha &= 2\zeta(w_\alpha/2), & \zeta(z) & \text{is the Zeta quasi periodic Weierstrass} \\ \text{function defined as } \zeta(z) &= \frac{1}{z} + \sum_{m,n}^{\infty} \left(\frac{1}{z - T_{nm}} + \frac{1}{T_{nm}} + \frac{z}{T_{nm}^2} \right), & \text{and the prime over the summation symbol means that the pair} & & & & \\ (m, n) &= (0, 0) \text{ is excluded. The Legendre's relationship links } \delta_1, \delta_2 \text{ and the periods } w_1, w_2: \delta_1 w_2 - \delta_2 w_1 = \pi i. \text{ The Laurent} & & & & & \\ \text{series expansion of } \zeta \text{ is } \zeta(z) &= \frac{1}{z} - \sum_{k=2}^{\infty} c_k \frac{z^{2k-1}}{2k-1}, \text{ where } c_1 = 0, c_2 = 3S_4, c_3 = 5S_6 \text{ and } c_k = \frac{3}{(2k+1)(k-3)} \sum_{m=2}^{k-2} c_m c_{k-m}, k \geq 4. \text{ The lattice} & & & & & \\ S_k & \text{is defined by } S_k = \sum_{m,n} (mw_1 + nw_2)^{-k}, m^2 + n^2 \neq 0, k > 2, S_2 = 0. \text{ In particular } S_4 \text{ and } S_6 \text{ used in the numerical} & & & & & \\ \text{implementation are reported in Table 1 of Ling and Tsai (1964) and Ling (1965) for parallelogram and rhombic cells} & & & & & & \\ \text{respectively.} & & & & & & \end{aligned}$$

The matrices \mathcal{N}_1 , \mathcal{P} and \mathcal{N}_2 are of infinite order and for the numerical implementation it is necessary to truncate to certain order $N \in \mathbb{N}$.

$$\text{The matrix } \mathcal{P} = \begin{pmatrix} P_{11} & \dots & P_{1N} \\ \vdots & \ddots & \vdots \\ P_{N1} & \dots & P_{NN} \end{pmatrix}_{4N \times 4N} \text{ is composed by sub-matrices } (P_{ts})_{4 \times 4}, \text{ defined by } P_{ts} = \delta_{ts}\mathcal{K} + \mathcal{M}_{ts},$$

$$\mathcal{M}_{ts} = \begin{pmatrix} \chi_\rho \begin{pmatrix} w_{12t+12s+1} & -w_{22t+12s+1} \\ -w_{22t+12s+1} & -w_{12t+12s+1} \end{pmatrix} & \chi_{s\rho}^- \begin{pmatrix} w_{12t+12s+1} & -w_{22t+12s+1} \\ -w_{22t+12s+1} & -w_{12t+12s+1} \end{pmatrix} \\ \chi_s \begin{pmatrix} w_{12t+12s+1} & -w_{22t+12s+1} \\ -w_{22t+12s+1} & -w_{12t+12s+1} \end{pmatrix} & \chi_{ts}^- \begin{pmatrix} w_{12t+12s+1} & -w_{22t+12s+1} \\ -w_{22t+12s+1} & -w_{12t+12s+1} \end{pmatrix} \end{pmatrix}, \quad w_{1kp} = \Re(w_{kp}), \quad w_{2kp} = \Im(w_{kp})$$

are the real and imaginary parts of the complex number $w_{kp} = \frac{(k+p-1)!}{(k-1)!(p-1)!} \frac{R^{k+p}}{\sqrt{kp}} S_{k+p}$, $k = 2t - 1$, $p = 2s - 1$, $t, s = 1, 2, 3 \dots$. The

matrices $\mathcal{N}_1 = (n_{41} \dots n_{4N})_{4 \times 4N}$ and $\mathcal{N}_2 = \begin{pmatrix} n_{14} \\ \vdots \\ n_{N4} \end{pmatrix}_{4N \times 4}$ are composed by sub-matrices $(n_{4t})_{4 \times 4}$ and $(n_{t4})_{4 \times 4}$ defined by

$n_{4k} = \mathcal{M}_{2t+1, 1}$, $n_{t4} = \mathcal{M}_{1, 2t+1}$ respectively.

3. Eigenfunction expansion-variational method (EEVM)

Recently Yan, Jiang, and Song (2011) presented a new variational functional for a unit cell of a heterogeneous solid with periodic microstructures by incorporating the quasi-periodicity of the displacement field and the periodicity of the stress and strain fields into the strain energy functional. The functional can accommodate a broad class of periodic structures. By combining with the eigenfunction expansions of the complex potentials satisfying the continuity conditions on the fiber–matrix interface, an Eigen-function expansion-variational method (EEVM) based on a unit cell is developed, which is also used to deal with fibrous elastic composite with general oblique cells for a comparison.

For the piezoelectric behavior considered here, the displacement field $u_i(\mathbf{x})$ and electrical potential field $\phi(\mathbf{x})$ are quasi-periodic, the stress field $\{\sigma_{13}(\mathbf{x}), \sigma_{23}(\mathbf{x})\}$ and electrical displacement field $\{D_1(\mathbf{x}), D_2(\mathbf{x})\}$ are periodic. For brevity and convenience, now introduce matrix notations for the variables as follows:

$$\begin{aligned} \mathbf{w} &= \begin{bmatrix} u_3 \\ \phi \end{bmatrix}, \quad \gamma_1 = \begin{bmatrix} 2\varepsilon_{13} \\ -E_1 \end{bmatrix}, \quad \gamma_2 = \begin{bmatrix} 2\varepsilon_{23} \\ -E_2 \end{bmatrix}, \quad \gamma = \begin{bmatrix} 2\varepsilon_{13} & 2\varepsilon_{23} \\ -E_1 & -E_2 \end{bmatrix}, \\ \boldsymbol{\tau}_1 &= \begin{bmatrix} \sigma_{13} \\ D_1 \end{bmatrix}, \quad \boldsymbol{\tau}_2 = \begin{bmatrix} \sigma_{23} \\ D_2 \end{bmatrix}, \quad \boldsymbol{\tau} = \begin{bmatrix} \sigma_{13} & \sigma_{23} \\ D_1 & D_2 \end{bmatrix}, \\ \nabla &= \begin{bmatrix} \frac{\partial}{\partial x_1} & \frac{\partial}{\partial x_2} \end{bmatrix}, \quad \mathbf{x} = \begin{bmatrix} x_1 \\ x_2 \end{bmatrix}, \quad \mathbf{L} = \begin{bmatrix} C_{44} & e_{15} \\ e_{15} & -\kappa_{11} \end{bmatrix}, \end{aligned} \quad (10)$$

where \mathbf{w} , γ and $\boldsymbol{\tau}$ are called generalized displacement, strain and stress, respectively.

From the doubly periodic distribution of unit cells shown in Fig. 1a, the boundary of a unit cell in Fig. 1b can be divided into ∂V_j^+ and ∂V_j^- in pairs ($j = 1, 2$). The loading condition of the composite can be prescribed by an average generalized strain over the unit cell, $\langle \gamma \rangle$, which is the same for every unit cell. The corresponding generalized displacements and tractions ($\mathbf{t} = \boldsymbol{\tau} \cdot \mathbf{n}$) on ∂V_k^+ and ∂V_k^- satisfy the following periodic boundary conditions:

$$\mathbf{w}^{k+} - \mathbf{w}^{k-} = \langle \varepsilon \rangle \cdot \mathbf{p}^k, \quad (11)$$

$$\mathbf{t}^{k+} + \mathbf{t}^{k-} = \mathbf{0}, \quad (12)$$

where $\mathbf{p}^1 = \{\text{Re} w_1, \text{Im} w_1\}$ and $\mathbf{p}^2 = \{\text{Re} w_2, \text{Im} w_2\}$, whereas $\mathbf{w}^{k+} - \mathbf{w}^{k-}$ denotes the generalized displacement difference between the opposite boundaries (see ∂V_k^+ and ∂V_k^- in Fig. 1b) of a unit cell.

By using the Lagrangian multiplier method, a generalized potential energy functional can be defined, and its stationary conditions, which is equivalent to the periodic boundary conditions, can be written as Rodriguez-Ramos et al. (2011)

$$\sum_s \int_{\partial V_s^+} \delta \mathbf{t}^{s+} \cdot (\mathbf{w}^{s+} - \mathbf{w}^{s-}) dS - \sum_s \int_{\partial V_s^+} (\mathbf{t}^{s+} + \mathbf{t}^{s-}) \cdot \mathbf{w}^{s-} dS = \sum_s \int_{\partial V_s^+} \delta \mathbf{t}^{s+} \cdot \langle \gamma \rangle \mathbf{p}^s dS, \quad (13)$$

where $\delta(\cdot)$ denotes the variation. The stationary conditions are suitable for a general unit cell with any microstructure, where symmetry and antisymmetry properties of the unit cell may not exist.

For the antiplane problem, the generalized displacement field $\mathbf{w}(\mathbf{x})$ satisfies Laplace's equation $\nabla^2 \mathbf{w} = \mathbf{0}$. It is seen that the generalized displacement \mathbf{w} , generalized stress $\boldsymbol{\tau}$ and generalized resultant force \mathbf{T} can be formulated by two potentials $\{f_1(z), f_2(z)\}$ with a vector form $\mathbf{f}(z)$:

$$\mathbf{w} = \frac{1}{2} [\mathbf{f}(z) + \overline{\mathbf{f}(z)}], \quad (14)$$

$$\boldsymbol{\tau}_1 - i\boldsymbol{\tau}_2 = \mathbf{L} \mathbf{f}'(z), \quad (15)$$

$$\mathbf{T} = \int_A^B \boldsymbol{\tau} \mathbf{n} dS = \frac{1}{2i} \mathbf{L} [\mathbf{f}(z) - \overline{\mathbf{f}(z)}]_A^B, \quad (16)$$

where the prime denotes the derivative with respect to z , $[\cdot]_A^B$ denotes the difference of the values of the bracketed function from point A to point B.

The complex potential $\mathbf{f}_f(z)$ in the fiber region can be expanded into a Taylor series and $\mathbf{f}_m(z)$ in the matrix region can be expanded into a Laurent series,

$$\mathbf{f}_f(z) = \sum_{n=1}^{\infty} \mathbf{C}_{1n} z^{2n-1}, \quad (17)$$

$$\mathbf{f}_m(z) = \sum_{n=1}^{\infty} \mathbf{C}_{2n} z^{-(2n-1)} + \sum_{n=1}^{\infty} \mathbf{C}_{3n} z^{2n-1}, \quad (18)$$

where \mathbf{C}_{1n} , \mathbf{C}_{2n} and \mathbf{C}_{3n} are complex coefficient vectors. Due to the centrosymmetry of the unit cell, only odd terms in (17) and (18) remain, which can be determined by using the fiber–matrix interface condition and the stationary condition (13). Then the generalized strain and stress tensors can be obtained from (14)–(16) and the effective properties of the composite L^e can be determined with the aid of the average field theory,

$$\langle \boldsymbol{\tau} \rangle = \mathbf{L}^e : \langle \boldsymbol{\gamma} \rangle, \quad (19)$$

where $\langle \boldsymbol{\tau} \rangle$ and $\langle \boldsymbol{\gamma} \rangle$ are the average generalized stress and strain tensors in a unit cell, respectively. Details about the numerical implementation can be found in Yan et al. (2011).

4. Analysis of results

The material parameters used in the computation are given in the following Table 1 where the abbreviate notation is used.

In this work different composite structures under suitable configurations of cells (Fig. 2) are studied. In order to determine the effective properties, the system of Eq. (8) is truncated in an appropriate order N , as w_{kp} depends on powers of radius R of the fiber; this ensures a rapid convergence to the exact solution. The calculations were made for $N = 10$. Comparison between AHM and EEVM are reported in order to validate both methods.

In Table 2 two phase composites Epoxy matrix/PZT-7A fiber with rectangular periodic cells ($w_1 = 1$, $w_2 = bi$ see Fig. 2a) is considered. The set of effective moduli C_{44}^* , e_{24}^* , κ_{22}^* decreases as the height of the rectangular cell increases. In other words, C_{44}^* , e_{24}^* , κ_{22}^* become stronger for small values of the height of the rectangular cell. On the other hand, C_{55}^* , e_{15}^* , κ_{11}^* increase as the height of the rectangular cell increases as well. This trend is due to the augment of the distance between the fibers in y_2 direction in this case of composite cell. The ratio of the piezoelectric coefficients in two directions, e_{15}^*/e_{24}^* , is over 7 as fiber volume fraction is 0.3 and $b = 2$. That is, the difference of distances between fibers in two directions can induce strong orthotropy of effective piezoelectric coefficients.

Fig. 3 illustrates the behavior of all normalized effective coefficients calculated by AHM and EEVM for two-phase composites Epoxy matrix/PZT-7A fiber with rhombic periodic cell for the volume fraction of the fiber $V_2 = 0.6$. The numerical results derived by AHM and EEVM are almost the same where the influence of the arrangement of the cells in the properties of the composite can be observed. The figure is grouped according to the following components: elastic, piezoelectric, dielectric and the set of overall properties derived from angles of the cell different of 60° and 90° (monoclinic class). All effective properties coincide at the angles 60° and 90° , i.e. $C_{44}^* = C_{55}^*$, $e_{24}^* = e_{15}^*$, $\kappa_{22}^* = \kappa_{11}^*$. The global properties of the composites are transversely isotropic at the angles 60° and 90° , the strongest anisotropy appears at angle 45° . In the range between 60° and 90° the trend of the curves of all coefficients are similar. The difference between the coefficients are remarkable for angles of the cell less than 60° . The explanation should be given due to the fact that in the short diagonal of the rhombic cell the distance between the fibers is small and it reinforces the properties of the composite in this direction. From Fig. 3 it can be observed that the effective properties (especially, C_{44}^* , e_{24}^* and κ_{22}^*) are considerably sensitive to the geometry of cells with varying the angle of the cells. For instance, $e_{24}^*/(C_{44}^{(1)}\kappa_{11}^{(1)})^{1/2}$ ranges from 0.6 to 0.2 with the angle of the cells varying from 45° to 90° .

In Table 3 a comparison of the effective properties between AHM and EEVM is shown for Epoxy/PZT-7A composite with parallelogram periodic cells. The global behavior of composites with periodic cells $w_1 = 1$, $w_2 = 1/2 + bi$ ($b = 1$, $b = 1.5$) is

Table 1
Material parameters.

Materials	C_{44} (GPa)	e_{15} (C/m ²)	κ_{11} (C/Vm)
Epoxy	1.8	0	0.0372
PZT-7A	25.7	9.35	4.065

Table 2
Composite with rectangular periodic cells ($w_1 = 1$, $w_2 = bi$ see Fig. 2a). Comparison between AHM and EEVM.

		Fiber volume fraction and $b = 1.1$			Fiber volume fraction and $b = 1.5$			Fiber volume fraction and $b = 2$		
		0.1	0.2	0.3	0.1	0.2	0.3	0.1	0.2	0.3
C_{55}^* (GPa)	AHM	2.172	2.643	3.259	2.190	2.741	3.589	2.214	2.895	4.307
	EEVM	2.172	2.643	3.259	2.190	2.741	3.589	2.214	2.895	4.307
e_{15}^* (C/m ²)	AHM	0.001571	0.004071	0.008271	0.001732	0.005134	0.01280	0.001959	0.007092	0.02724
	EEVM	0.001571	0.004071	0.008271	0.001732	0.005134	0.01280	0.001959	0.007092	0.02724
κ_{11}^* (C/Vm)	AHM	0.04549	0.05615	0.07048	0.04592	0.05859	0.07901	0.04649	0.06251	0.09930
	EEVM	0.04549	0.05615	0.07048	0.04592	0.05859	0.07901	0.04649	0.06251	0.09930
C_{44}^* (GPa)	AHM	2.163	2.596	3.126	2.147	2.526	2.943	2.131	2.458	2.789
	EEVM	2.163	2.596	3.126	2.147	2.526	2.943	2.131	2.458	2.789
e_{24}^* (C/m ²)	AHM	0.001491	0.003618	0.00676	0.001361	0.002984	0.004979	0.001229	0.002437	0.003717
	EEVM	0.001491	0.003618	0.00676	0.001361	0.002984	0.004979	0.001229	0.002437	0.003717
κ_{22}^* (C/Vm)	AHM	0.04526	0.05502	0.06715	0.04489	0.05333	0.06271	0.04450	0.05171	0.05904
	EEVM	0.04526	0.05502	0.06715	0.04489	0.05333	0.06271	0.04450	0.05171	0.05904

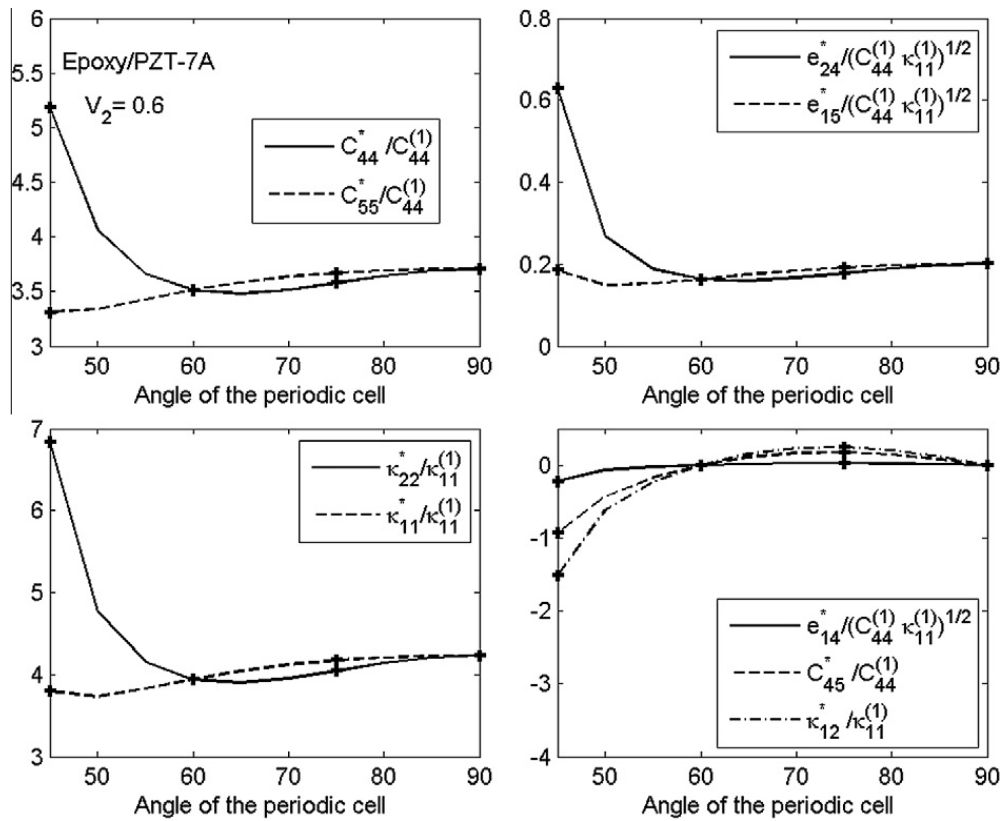


Fig. 3. Effective properties by AHM and EEVM (with symbol “+”) for two-phase composites with rhombic periodic cell ($w_1 = 1$, $w_2 = e^{i\theta}$, see Fig. 2b).

Table 3

Effective properties of composites with parallelogram cells ($w_1 = 1$, $w_2 = 1/2 + bi$ see Fig. 2c).

V_2		$b = 1$				$b = 1.5$		
		0.1	0.3	0.5	0.7	0.1	0.3	0.5
C_{44}^* (GPa)	AHM	2.16	3.14	4.69	7.63	2.15	2.94	3.96
	EEVM	2.16	3.14	4.69	7.63	2.15	2.94	3.96
C_{55}^* (GPa)	AHM	2.17	3.24	5.20	10.55	2.19	3.59	9.88
	EEVM	2.17	3.24	5.20	10.55	2.19	3.59	9.88
e_{15}^* (C/m ²)	AHM	0.00	0.01	0.03	0.16	0.00	0.01	0.26
	EEVM	0.00	0.01	0.03	0.16	0.00	0.01	0.26
e_{24}^* (C/m ²)	AHM	0.00	0.01	0.02	0.06	0.00	0.00	0.01
	EEVM	0.00	0.01	0.02	0.06	0.00	0.00	0.01
κ_{11}^* (nC/Vm)	AHM	0.05	0.07	0.12	0.28	0.05	0.08	0.30
	EEVM	0.05	0.07	0.12	0.28	0.05	0.08	0.30
κ_{22}^* (nC/Vm)	AHM	0.05	0.07	0.10	0.18	0.04	0.06	0.09
	EEVM	0.05	0.07	0.10	0.18	0.04	0.06	0.09

orthorhombic of class 2 mm. The percolation limit, i.e. the volume when the fibers are in contact, changes according with the configuration of the cells. For instance, the case $b = 1.5$ requires maximal percolation limit of $V_2 = 0.52$, whereas the case $b = 1$ the percolation limit is $V_2 = 0.785$. Notice that all effective properties increase as the fiber volume fraction increases as well. Similar to the case of the rectangular periodic cell, the difference of the density of fibers in two directions induces anisotropy of the effective moduli. Furthermore, the piezoelectric coefficient shows stronger anisotropy than the elastic coefficient and dielectric coefficient do.

A piezoelectric porous medium with aligned voids can be regarded as a composite with empty fibers. The global properties of the composite with empty fibers and PZT-7A matrix with parallelogram cell ($w_1 = 1$, $w_2 = 1/2 + 0.2i$ see Fig. 2c) are shown in Table 4. The effective properties of porous composite are normalized by the matrix materials constants. The table shows that the expressions derived in the present models (7) and (19) can effectively describe a piezoelectric porous medium with aligned voids (permittivity of air $k = 8.86 \times 10^{-12}$ C/Vm), taking the fibers properties as zero (10^{-10}).

Table 4

Effective properties for PZT-7A/porous piezoelectric composite with parallelogram periodic cell.

V_2	0.1		0.2		0.3		0.4		0.5		0.6	
	AHM	EEVM	AHM	EEVM	AHM	EEVM	AHM	EEVM	AHM	EEVM	AHM	EEVM
$C_{55}^*/C_{44}^{(1)}$	0.81	0.81	0.65	0.65	0.50	0.50	0.37	0.37	0.24	0.24	0.09	0.09
$e_{15}^*/e_{15}^{(1)}$	0.81	0.81	0.65	0.65	0.50	0.50	0.37	0.37	0.24	0.24	0.09	0.09
$\kappa_{11}^*/\kappa_{11}^{(1)}$	0.81	0.81	0.65	0.65	0.50	0.50	0.37	0.37	0.24	0.24	0.09	0.10
$C_{44}^*/C_{44}^{(1)}$	0.82	0.82	0.68	0.68	0.57	0.57	0.47	0.47	0.39	0.39	0.32	0.32
$e_{24}^*/e_{15}^{(1)}$	0.82	0.82	0.68	0.68	0.57	0.57	0.47	0.47	0.39	0.39	0.32	0.32
$\kappa_{22}^*/\kappa_{11}^{(1)}$	0.82	0.82	0.68	0.68	0.57	0.57	0.47	0.48	0.39	0.39	0.32	0.32

The computation by the presented models shows total coincidence with the results reported in Bravo-Castillero et al. (2009). Notice from Table 4 that for the same fiber volume fraction the ratios $\frac{C_{55}^*}{C_{44}^{(1)}} = \frac{e_{15}^*}{e_{15}^{(1)}} = \frac{\kappa_{11}^*}{\kappa_{11}^{(1)}}$, $\frac{C_{44}^*}{C_{44}^{(1)}} = \frac{e_{24}^*}{e_{15}^{(1)}} = \frac{\kappa_{22}^*}{\kappa_{11}^{(1)}}$ and $\frac{C_{55}^*}{C_{44}^{(1)}} = \frac{e_{15}^*}{e_{24}^*} = \frac{\kappa_{11}^*}{\kappa_{22}^*}$ are constants, see formulae (29) of Bravo-Castillero et al. (2009). All effective properties decrease, showing that the composite becomes weaker as the porosity increasing. Moreover, the same values of Table 4 can be obtained if the following materials parameters in formulae (9) are reduced to $\chi_\rho = \chi_s = 1$, $\chi_{sp}^+ = \chi_{sp}^- = E^{(1)}$, $\chi_{ts}^+ = \chi_{ts}^- = -1/E^{(1)}$.

On the other hand, the Schulgasser's universal relations reported by Schulgasser (1992) for transversely isotropic composites can be numerically verified from (7) and (19). These universal relations have been modified to piezoelectric composites with parallelogram periodic cells and they can be written in the following form,

$$\begin{vmatrix} C_{55}^* - iC_{45}^* & C_{55}^{(1)} & C_{55}^{(2)} \\ e_{15}^* - ie_{25}^* & e_{15}^{(1)} & e_{15}^{(2)} \\ \kappa_{11}^* - i\kappa_{12}^* & \kappa_{11}^{(1)} & \kappa_{11}^{(2)} \end{vmatrix} = 0; \quad \begin{vmatrix} C_{54}^* - iC_{44}^* & C_{44}^{(1)} & C_{44}^{(2)} \\ e_{14}^* - ie_{24}^* & e_{24}^{(1)} & e_{24}^{(2)} \\ \kappa_{21}^* - i\kappa_{22}^* & \kappa_{22}^{(1)} & \kappa_{22}^{(2)} \end{vmatrix} = 0.$$

The importance of these relations consists to minimize the quantity of effective coefficients to be calculated. For instance, by AHM the number of local problems to be solved are reduced to two problems, in particular, L_{13} and L_{23} . Besides, this relation allows numerical benchmark for validation of models.

5. Conclusions

In this work closed analytic expressions for two-phase fibrous periodic composites with parallelogram cells are derived using two different approaches. The configuration of the cells related to the anisotropy of the composite is illustrated. In general, the composite belongs to monoclinic symmetric class characterized by 9 homogenized coefficients. Using these models the porous effective properties can be estimated as a limit case. The Schulgasser's universal relations are numerically tested.

Both methods almost give the same results for all volume fractions in all configurations of the cells. The distribution of fibers with different density in two directions can induce strong anisotropy of the effective moduli, and the piezoelectric coefficient shows stronger anisotropy than the elastic coefficient and dielectric coefficient do.

Acknowledgements

The funding of Conacyt project number 129658, the National Natural Science Foundation of China under Grant NNSFC 10972020, and the Fundamental Research Funds for the Central Universities are gratefully acknowledged. Thanks to Ramiro Chávez Tovar and Ana Pérez Arteaga for computational assistance.

References

- Artoli, E., Bisegna, P., & Maceri, F. (2010). Effective longitudinal shear moduli of periodic fibre-reinforced composites with radially-graded fibres. *International Journal of Solids and Structures*, 47, 383–397.
- Boyd, J. G., Lagoudas, D. C., & Seo, C. S. (2003). Arrays of micro-electrodes and electromagnets for processing of electromagneto-elastic multifunctional composite materials. In *SPIE 10th annual international symposium on smart structures held at San Diego, CA, March 2–6* (Vol. 5055, pp. 268–277).
- Bravo-Castillero, J., Guinovart-Díaz, R., Sabina, F. J., & Rodríguez-Ramos, R. (2001). Closed-form expressions for the effective coefficients of fibre-reinforced composite with transversely isotropic constituents-II. Piezoelectric and square symmetry. *Mechanics of Materials*, 33, 237–248.
- Bravo-Castillero, J., Rodríguez-Ramos, R., Guinovart-Díaz, R., Sabina, F. J., Aguiar, A. R., Silva, U. P., et al. (2009). Analytical formulae for electromechanical effective properties of 3-1 longitudinally porous piezoelectric materials. *Acta Materialia*, 57, 795–803.
- Golovchan, V. T., & Nikityuk, N. I. (1981). Solution of the problem of shear of a fibrous composite medium. *Translated from Prikladnaya Mekhanika*, 17(2), 29–35.
- Guinovart-Díaz, R., López-Realpozo, J. C., Rodríguez-Ramos, R., Bravo-Castillero, J., Ramírez, M., Camacho-Montes, H., et al. (2011). Influence of parallelogram cells in the axial behaviour of fibrous composite. *International Journal of Engineering Science*, 49, 75–84.
- Ling, C.-B. (1965). Evaluation at half periods of Weierstrass' elliptic functions with double periods 1 and $e^{i\alpha}$. *Mathematics of Computation*, 19(92), 658–661.

- Ling, C.-B., & Tsai, C.-P. (1964). Evaluation at half periods of Weierstrass' elliptic function with rhombic primitive period parallelogram. *Mathematics of Computation*, 18(87), 433–440.
- Molkov, B. A., & Pobedria, B. E. (1985). Effective characteristic of fibrous unidirectional composite with periodic structure. *Mechanic of Solids*, 2, 119–129 (in Russian).
- Nabi, A., Abhay, N., Ghodrat, K., & Chad, U. (2008). A micromechanical characterization of angular bidirectional fibrous composites. *Computational Materials Science*, 43, 1193–1206.
- Rodríguez-Ramos, R., Yan, P., Lopez-Realpozo, J. C., Guinovart-Díaz, R., Bravo-Castillero, J., Sabina, F. J., et al (2011). Two analytical models for the study of periodic fibrous elastic composite with different unit cells. *Composite Structures*, 93, 709–714.
- Royer, D., & Dieulesaint, E. (2000). *Elastic waves in solids I*. Berlin, Heidelberg: Springer Verlag.
- Sabina, F. J., Rodríguez-Ramos, R., Bravo-Castillero, J., & Guinovart-Díaz, R. (2001). Closed-form expressions for the effective coefficients of fibre-reinforced composite with transversely isotropic constituents-II. Piezoelectric and hexagonal symmetry. *Journal Mechanics of Physics of Solids*, 49, 1463–1479.
- Schulgasser, K. (1992). Relationship between the effective properties of transversely isotropic piezoelectric composites. *Journal of the Mechanics of Physics and Solids*, 40, 473.
- Yan, P., & Jiang, C. P. (2010). An eigenfunction expansion-variational method based on a unit cell in analysis of a generally doubly-periodic array of cracks. *Acta Mechanica*, 210(1-2), 117–134.
- Yan, P., Jiang, C. P., & Song, F. (2011). An eigenfunction expansion-variational method for the anti-plane electroelastic behavior of three-phase fiber composites. *Mechanics of Materials*, 43(10), 586–597.
- Yan, P., Jiang, C. P., Song, F., & Xu, X. H. (2010). Estimation of transverse thermal conductivity of doubly-periodic fiber reinforced composites. *Chinese Journal of Aeronautics*, 23(1), 54–60.